Available online at www.sciencedirect.com
SCIENCE DIRECT®
Physica A 367 (2006) 461–478
PHYSICA A
www.elsevier.com/locate/physa

A composite traffic flow modeling approach for incident-responsive network traffic assignment

Jiuh-Biing Sheu*

Institute of Traffic and Transportation, National Chiao Tung University, 4F, 114 Chung Hsiao W. Rd., Sec. 1, Taipei, Taiwan 10012, Taiwan, ROC

Received 31 October 2003; received in revised form 25 October 2005
Available online 27 December 2005

Abstract

This paper presents a hybrid traffic simulation-based model to address the network traffic route choice issue under conditions of lane-blocking incidents on surface streets. The proposed approach includes four sequential mechanisms: (1) link flow loading, (2) link traffic moving, (3) link cost calculation, and (4) searching the shortest path. To deal with the traffic flows moving on lane-blocking links, specific incident-induced link traffic flow models, which are extended from the Lighthill–Whitham (L–W for short) model, are formulated. A simulation-based approach is then proposed to determine the instantaneous shortest path associated with each vehicle approaching to each given intersection on the network. In addition, numerical examples associated with diverse incident scenarios are investigated. The numerical results demonstrate the competitiveness of the proposed simulation-based method by reducing the network-wide path travel time by 11.4% and the incident impact on link traffic flows by 66.7% in comparison with the Paramics traffic simulator. It is expected that this study can provide linkage between the fields of incident management and dynamic traffic assignment that will allow the development of such related technologies as real-time incident-responsive route guidance and incident management systems.
© 2005 Elsevier B.V. All rights reserved.

Keywords: Traffic simulation; Route choice; Incident-induced traffic congestion; Incident-responsive; Lighthill–Whitham model; Traffic assignment

1. Introduction

Incident-responsive in-vehicle route guidance (RG) remains challenging in the field of dynamic traffic assignment (DTA), for the following three major reasons. First, in previous research, incident-induced intra-lane and inter-lane traffic maneuvers have been proved to be significantly different from incident-free lane traffic behavior [1–4]. Thus, they have an unusual impact on the link capacity, which is commonly regarded as one of important factors in determining the link cost of DTA. For instance, there is an argument that once a lane is blocked in a 3-lane link, the link capacity can be reduced by more than one-third, and the reduction

*Tel.: +886 2 2349 4963; fax: +886 2 2349 4953.
E-mail address: jbsheu@mail.nctu.edu.tw.

0378-4371/$ - see front matter © 2005 Elsevier B.V. All rights reserved.
doi:10.1016/j.physa.2005.11.039

may differ with the spatial and temporal attributes of incidents such as incident location and duration, respectively. Second, the first-in-first-out (FIFO) presumption which is postulated in numerous published DTA algorithms may no longer hold true under lane-blocking incident conditions due to the phenomenon of incident-induced mandatory lane changes occurring upstream from the incident site. One striking example is that any further upstream new arrivals of vehicles present in the blocked lane may conduct lane-changing maneuvers earlier than the vehicles queuing ahead to pass smoothly by the incident site. Consequently, the FIFO prerequisite is violated in this case. Third, the effects of the incident on drivers' decisions in terms of route choice remain ambiguous. Given that one lane is blocked on a given multi-lane link in the shortest path, it is not surprising that some drivers may still follow the shortest path to complete their trips, but some aggressive drivers may change routes even if the original path with the incident is shorter than others. Similar arguments and further elaborate discussion can also be found in Ref. [5].

Although remarkable advances can be found in previous literature to improve the validity of DTA in various ITS-induced traffic environments, the effectiveness of the existing DTA algorithms in terms of their potential for redistributing network flows under lane-blocking incident conditions remains problematic. In general, the published DTA approaches can be classified into four groups including: (1) mathematical programming, (2) optimal control, (3) variation inequality (VI), and (4) simulation. Below we illustrate some typical algorithms to indicate the limitations of the existing DTA algorithms for incident cases.

The mathematical programming-based DTA approach originated from the Merchant–Nemhauser (M–N) model [6,7]. It was then reformulated by Carey [8] as a convex nonlinear model which incorporates the variable of the actual link exit flow. Subsequently, much improvement can be found in Refs. [9,10], both of which formulate the dynamic user equilibrium (UE) problem as a link-based bi-level program. Even so, the validity of the static outbound link-flow function as the link-flow service rate set in these published models is problematic under conditions of lane-blocking incidents.

The idea of utilizing optimal control theories in dealing with DTA problems was initiated in Ref. [11], and extensively investigated in Ref. [12], both of which contributed to the goal of coordinating the ITS-related technologies of real-time traffic control and dynamic RG systems, as did in some literature [13,14]. One distinctive characteristic exhibited in numerous existing optimal control-based DTA approaches [12,15–19] is that either or both the link inflow and the link outflow are regarded as time-varying control variables to serve the goal of minimizing the total link cost. Nevertheless, the difficulty in specifying the vague relationship between the time-varying control and state variables under lane-blocking incident conditions together with the burdensome computational requirements in searching for the optimal solution are significant issues remaining in the existing optimal control-based DTA models.

Both Friesz et al. [20] and Smith [21] can be regarded as two pioneer studies with respect to the VI-based DTA approach, which has been proved to be useful particularly for formulating the complex simultaneous route and departure time choice problem. Since then, there have been many attempts to improve the VI-based DTA approach in efficiently obtaining an approximate solution via various computational algorithms, e.g., heuristic algorithms [22–25]. Nevertheless, such incident-induced lane traffic phenomena as mandatory lane changing and queuing can make the link flow dynamics more complex than expected in these existing VI-based models, and thus lead to biased solutions. Similar issues are also found in Ref. [26], in which the spatial queue dynamics in the presence of an incident cannot be characterized.

As for the simulation-based DTA approach, recent years have seen an increasing interest in incorporating ATMS/ATIS technologies with such models as CONTRAM [27,28], INTEGRATION [29], DYNASMART [30–33], and DYNAMIT, all which are well-known traffic-assignment simulators, to systematically assess the performance of traffic networks. Furthermore, several evaluations of alternative control-assignment simulation models have been recently reported in Refs. [34–36] to investigate issues relevant to the equilibrium of network flows under diverse signal control strategies. Other simulation approaches to addressing specific DTA-related issues can also be found in the literature [37–40].

Despite the advantage of the simulation-based DTA approach in terms of characterizing traffic control effects on link flow dynamics in comparison with the other DTA approaches, the feasibility of link traffic flow models embedded in the existing simulation-based DTA approaches warrant further investigations. For instance, the routing logic of INTEGRATION does not directly respond to the occurrence of an incident. Instead, it responds indirectly to the incident delay. It is also worth noting that the incident severity referring

to the reduction of link capacity should also be predetermined in INTEGRATION; however such an incident-impact index in reality is time-varying, and hard to be preset because it changes with traffic flow conditions. In this aspect, it seems more agreeable that once an incident occurs, an advanced DTA method should be capable of responding to incident impacts as soon as possible rather than relies on the severity of the unexpected incident-induced delays, as did by INTEGRATION. DYNASMART is regarded advanced in many aspects of network-wide DTA, particularly in the aspect of integrating both traffic control and traveler information models with the embedded DTA algorithm in an attempt to solve network-wide traffic assignment problems through integrated ATMIS technologies. However, there are limited test results to show the capability of DYNASMART in dealing with diverse incident impacts on link traffic flows, which must rely to a certain extent on feasibility of the embedded macroscopic traffic flow models under various lane-blocking incident conditions. For instance, shock wave theories may not be suitable for uses under conditions of lane-blocking incidents on surface streets, particularly in cases of short blocks, different lanes existing in the mainline link segment and the following approach, and disturbance resulting from signal control. Any other macroscopic traffic flow models embedding continuous flow functions may also face similar problems for surface street incident cases. Accordingly, the link travel times estimated by DYNASMART in the presence of surface street lane-blocking incidents may be problematical for further use in incident-responsive traffic assignment and signal control.

In addition to the aforementioned approaches, several attempts have been made to investigate link traffic dynamics for addressing specific issues existing in DTA. Through an elaborate overview on time-dependent link travel time functions, Ran et al. [41] suggested two sets of link travel time functions including stochastic and deterministic functions for DTA on signalized networks, where physical constraints on link flows are introduced in their approach to deal with the vehicular spillback problem. Nevertheless, the variety of incident characteristics, as well as the incident effect on inter-lane and intra-lane traffic flows, may lead to difficulty in determining the upper bound in terms of the number of vehicles accommodated by the incident-impacted link in their approach. Utilizing equilibrium link flow models, the issue of spatial effect of queue spillovers on route choice is investigated in Ref. [5]. However, time-dependent traffic assignment with queue overflows remains as an unsolved problem in this literature.

It is also noteworthy that some improved traffic assignment algorithms such as quasi-dynamic and path-based traffic assignment models may save computational time; however, the distinctive methodological attributes of the aforementioned approaches in responding to either the temporal or the spatial traffic flow patterns on networks may lead these models to fail under lane-blocking incident conditions. Those so-called quasi-DTA models (e.g., Refs. [42,43]) mainly rely on the change patterns of daily origin–destination (O–D) traffic flows to formulate hourly period time-dependent traffic assignment problems, and thus, may not be able to respond to short-term changes of link flow patterns caused by incidents. In contrast with the temporal properties of quasi-DTA models, published path-based traffic assignment models (e.g., Refs. [32,44]) may also fail to respond to lane-blocking incidents in the process of traffic assignment because of their spatial limitations in characterizing the time-varying incident effect on link travel cost. One typical issue that may exist in the published path-based DTA models is the determination of the shortest paths on a given network in response to the effect of incident-induced traffic congestion on these path traffic flows.

The main point of the above literature review is the importance of recognizing the linkage between DTA and incident management for efficiently solving incident-induced traffic congestion problems in urban areas. In this regard, previous studies appear inadequate in in-depth understanding of incident effects on network traffic assignment, from either a microscopic or from a macroscopic point of view. Correspondingly, the incident-induced link travel cost and its influence on network-wide drivers' route choices are not incorporated in the prior literature, and thus, form the main limitations of the published DTA technologies applying to incident cases.

Accordingly, in this paper, a simulation-based approach is proposed to deal with network-wide in-vehicle route choice problem under conditions of lane-blocking incidents on surface streets. The architecture of the proposed approach is presented in Section 2 which includes the formulation of the proposed dynamic prediction models of incident-induced link costs. Section 3 illustrates a numerical example to demonstrate the effectiveness of the proposed method. Concluding remarks are then summarized in Section 4.

2. Description of the model

The proposed approach is presently limited to solving the UE route choice problems under conditions of lane-blocking incidents on surface streets. Let us consider a traffic network with multiple O–D, represented by given sets of nodes and directed links. For simplification of model formulation, the following basic assumptions are postulated:

(1) The time-dependent O–D demands and information on incident location are given.
(2) Only lane-blocking incidents on links are assumed.
(3) The incident effect on the pre-trip driver behavior, e.g., the departure time, is not taken into account.
(4) All drivers of the network are perfectly informed with road traffic conditions and follow information in terms of the instantaneous shortest path provided by the proposed system.

Then, we propose an incident-responsive simulation-assignment framework, shown in Fig. 1, which consists of four major mechanisms: (1) link flow loading, (2) link traffic moving, (3) link cost calculation, and (4) searching for the shortest path. In the process of incident-responsive DTA, these four mechanisms are sequentially executed in any given time interval.

Note that the aforementioned four-procedure routine is repeated in each time interval until all the given time-varying O–D traffic flows run though the associated instantaneous shortest paths. Through the four mechanisms executed in the proposed method, each link traveled by a given vehicle is traced until the given vehicle arrives at the corresponding final destination. Then the aggregate path formed by these corresponding traced links, referring to the simulation-based shortest path, is assigned to the corresponding given vehicle for its routing in the traffic network. It should also be noted that here the instantaneous shortest path associated with each vehicle is determined by the estimated path travel time which is aggregated by link travel times. Therefore, no matter what degree a link is affected by an incident with, the corresponding link travel time will be estimated using the proposed model, and then taken into account in the procedure of searching for the instantaneous shortest path. Because any link travel time here is time-varying, the instantaneous shortest path associated with each vehicle is updated each time when the given vehicle is approaching to an intersection being reassigned to the next link. Accordingly, one typical example is that the more severe the incident-induced traffic congestion is on the incident link at a given time step, the fewer vehicles from the preceding links are assigned to the incident link at that moment, and vice versa.

The models embedded in these mechanisms are described below.

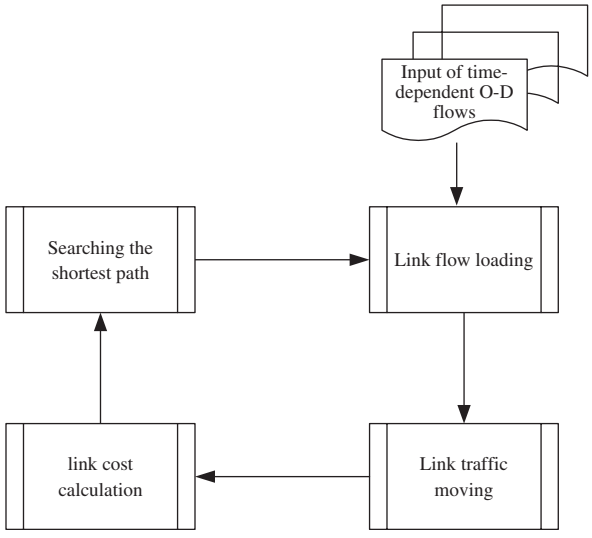

Fig. 1. Framework of incident-responsive simulation-assignment model.

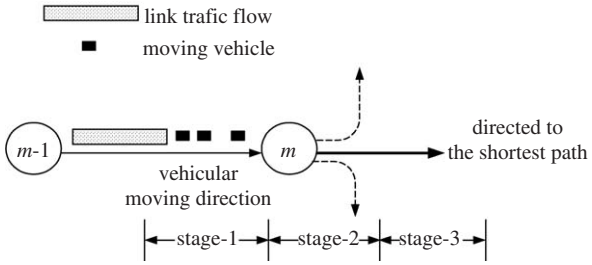

Fig. 2. The procedure of link flow loading.

2.1. Link flow loading

This mechanism serves to assign vehicles approaching from each given node to the following links in a given time interval k with the principle that each vehicle keeps moving on the instantaneous shortest path until arriving at its destination. Herein, three sequential stages are involved, as shown in Fig. 2. Given a link traffic flow moving to a given node m from the upstream node $m-1$ in a given time interval k, the portion of the flow present on the approach of the node m is decomposed into microscopic vehicles in Stage 1, where each vehicle is associated with a unique code in sequence. Stage 2 then searches for all the potential paths from the given node m to the destination for each approaching vehicle, and determines the associated instantaneous shortest path by summing up the estimated instantaneous total travel time spent on the links and nodes in each given path candidate. Simply, the node travel time is estimated according to the average delay induced by the signal effect, and depends on the type of the signal control mode implemented at that intersection. By contrast, the estimation of time-varying link travel time is quite a complex procedure in the study scope, and thus, is detailed in the following subsections. According to the instantaneous shortest paths determined in Stage 2, these approaching vehicles are then reloaded to the next links in Stage 3; and meanwhile, join the traffic flows presented in the next links.

2.2. Link traffic moving

This mechanism uses macroscopic traffic flow models to simulate the network-wide link traffic movement, considering two scenarios: traffic moving on incident-impacted links and on incident-free links. For simulating incident-free link traffic flows, we readily employ the L–W model [45] that has been successfully applied to capture macroscopic intra-lane traffic flow behavior in most incident-free traffic congestion cases. The L–W model basically consists of a conservation equation, as shown in Eq. (1), describing the intra-lane dynamics of the point density $\rho(x,t)$ in relation to the point flow $q(x,t)$.

$$\frac{\partial q(x,t)}{\partial x}+\frac{\partial \rho(x,t)}{\partial t}=0, \tag{1}$$

where $q(x,t)$ represents the instantaneous traffic flow observed at point (x,t) in vehicles per unit time; and $\rho(x,t)$ refers to the instantaneous traffic density measured at point (x,t) in vehicles per unit distance. Both $q(x,t)$ and $\rho(x,t)$ are dynamic with respect to space (x) and time (t), and correspondingly, they are functions of x and t in the L–W model. By contrast, unexpected bias may arise in characterizing incident-impacted traffic flow behavior if the published traffic flow models are used directly, as we noted previously [3,46]. Therefore, we propose a modified L–W model particularly for moving link traffic flows under incident conditions. The details of the model are described below.

Given a lane blockage occurring in a given lane of a three-lane link, the intra-lane equilibrium condition exhibited in Eq. (1) may no longer hold true due to the significant existence of lane-changing maneuvers, including (1) mandatory lane changing, and (2) discretionary lane changing, in the presence of lane-blocking incidents. Herein, mandatory lane changing is defined as the vehicular lane-changing behavior forced by such unexpected events as lane-blocking incidents, and it may exist significantly in the blocked lane upstream to the incident site. By contrast, the discretionary lane changing may significantly occur downstream to the incident

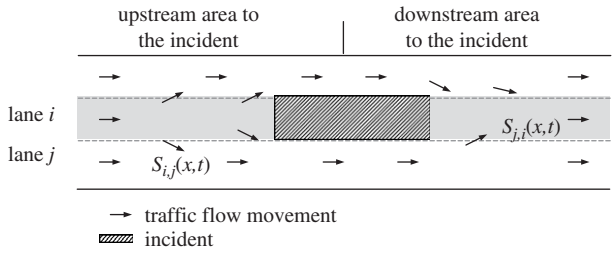

Fig. 3. Incident-induced non-equilibrium conditions of lane traffic flows.

site, particularly from adjacent lanes to the blocked lane. Such incident-induced traffic phenomena are illustrated in Fig. 3 from a macroscopic point of view. Therefore, for each given lane i of the given incident-impacted link $\bar{l}$, we revise the L–W model as

$$\frac{\partial q_i^{\bar{l}}(x,t)}{\partial x}+\frac{\partial \rho_i^{\bar{l}}(x,t)}{\partial t}=\sum_{\forall j} s_{j,i}^{\bar{l}}(x,t)-s_{i,j}^{\bar{l}}(x,t), \tag{2}$$

where $q_i^{\bar{l}}(x,t)$ and $\rho_i^{\bar{l}}(x,t)$ are the dynamics of the flow and density associated with the given lane i of the incident-impacted link $\bar{l}$; $s_{i,j}^{\bar{l}}(x,t)$ and $s_{j,i}^{\bar{l}}(x,t)$ are the unit inter-lane flows from the given lane i to a given adjacent lane j, and from the adjacent lane j to the given lane i, respectively. The mathematical forms of $s_{i,j}^{\bar{l}}(x,t)$ and $s_{j,i}^{\bar{l}}(x,t)$ are expressed as

$$s_{i,j}^{\bar{l}}(x,t)=\frac{\rho_i^{\bar{l}}(x,t)\times p_{i,j}^{\bar{l}}(x,t)}{d_{i,j}^{c}}, \tag{3}$$

$$s_{j,i}^{\bar{l}}(x,t)=\frac{\rho_j^{\bar{l}}(x,t)\times p_{j,i}^{\bar{l}}(x,t)}{d_{j,i}^{c}}, \tag{4}$$

where $p_{i,j}^{\bar{l}}(x,t)$ and $p_{j,i}^{\bar{l}}(x,t)$ represent the dynamics of lane-changing probabilities from lane i to lane j, and from lane j to lane i, respectively, occurring in the incident-impacted link $\bar{l}$; $d_{i,j}^{c}$ and $d_{j,i}^{c}$ are the average values of time spent in lane-changing maneuvers from lane i to lane j, and from lane j to lane i, respectively; similar to $\rho_i^{\bar{l}}(x,t)$, $\rho_j^{\bar{l}}(x,t)$ represents the dynamics of the density associated with the given lane j of the incident-impacted link $\bar{l}$. Herein, the inter-lane dynamics, $s_{i,j}^{\bar{l}}(x,t)$ and $s_{j,i}^{\bar{l}}(x,t)$, shown in Eq. (2) have not yet been determined because both $p_{i,j}^{\bar{l}}(x,t)$ and $p_{j,i}^{\bar{l}}(x,t)$ are unknown, according to Eqs. (3) and (4). We therefore propose the following logic rules for estimating these lane-changing dynamics under the conditions of mandatory and discretionary lane-changing maneuvers.

In the proposed method, two major factors are considered in determining the lane-changing dynamics: (1) the time-varying longitudinal spacing between the incident site to the targeted platoon approaching upstream to the incident site, and (2) the relative traffic conditions in adjacent lanes. In the case of mandatory lane changing, which generally occurs in the blocked lane upstream from the incident site, both the aforementioned spacing and traffic factors are involved in estimating the mandatory lane-changing dynamics ($p_{i,j}^{\bar{l}_{mc}}(x,t)$) with the following logic:

$$p_{i,j}^{\bar{l}_{mc}}(x,t)=\tilde{p}_{i,j}^{\bar{l}_{sf}}(x,t)\times\tilde{p}_{i,j}^{\bar{l}_{tf}}(x,t), \tag{5}$$

where $\tilde{p}_{i,j}^{\bar{l}_{sf}}(x,t)$ and $\tilde{p}_{i,j}^{\bar{l}_{tf}}(x,t)$ represent the dynamics of the possibilities with which the targeted platoon conducts mandatory lane-changing maneuvers under the existing conditions of approaching-incident spacing and adjacent-lane traffic in the incident-impacted link $\bar{l}$, coded with $\bar{l}_{sf}$ and $\bar{l}_{tf}$, respectively. Herein, $\tilde{p}_{i,j}^{\bar{l}_{sf}}(x,t)$ is

supposed to have the negative exponential relationship with the platoon-incident spacing ($x_{\bar{l}_{sf}}$); simply, $\tilde{p}_{i,j}^{\bar{l}_{tf}}(x,t)$ is assumed to follow the multinomial logit-like lane choice behavior [47] by comparing the traffic conditions among the adjacent lanes. Thus, we have $\tilde{p}_{i,j}^{\bar{l}_{sf}}(x,t)$ and $\tilde{p}_{i,j}^{\bar{l}_{tf}}(x,t)$ further expressed as

$$\tilde{p}_{i,j}^{\bar{l}_{sf}}(x,t) = \mathrm{e}^{-ax_{\bar{l}_{sf}}}, \tag{6}$$

$$\tilde{p}_{i,j}^{\bar{l}_{tf}}(x,t) = \frac{\mathrm{e}^{-b\rho_j(x,t)}}{\sum_{\forall \hat{j}\in\bar{l}}\mathrm{e}^{-b\rho_j(x,t)}}, \tag{7}$$

where $\hat{j}$ represents any given lane in incident-impacted link $\bar{l}$; a and b are two predetermined parameters. Combining Eqs. (6) and (7) with Eq. (5), we then have the following generalized form estimating the dynamics of mandatory lane-changing probability ($p_{i,j}^{\bar{l}_{mc}}(x,t)$) from a given lane i to the adjacent lane j in a given incident-impacted link $\bar{l}$:

$$p_{i,j}^{\bar{l}_{mc}}(x,t) = (\mathrm{e}^{-ax_{\bar{l}_{sf}}}) \times \left[\frac{\mathrm{e}^{-b\rho_j(x,t)}}{\sum_{\forall \hat{j}\in\bar{l}}\mathrm{e}^{-b\rho_j(x,t)}}\right]. \tag{8}$$

By contrast, only the factor of the relative traffic conditions in adjacent lanes is taken into account in estimating the discretionary lane-changing dynamics. Similarly, the hypothesis of the logit-like lane choice behavior is postulated, and thus the dynamics of the discretionary lane-changing probability from a given lane i to a given adjacent lane j in the given incident-impacted link $\bar{l}$ ($p_{i,j}^{\bar{l}_{dc}}(x,t)$) are given by

$$p_{i,j}^{\bar{l}_{dc}}(x,t) = \frac{\mathrm{e}^{-b\rho_j(x,t)}}{\sum_{\forall \hat{j}\in\bar{l}}\mathrm{e}^{-b\rho_j(x,t)}}. \tag{9}$$

Accordingly, the following traffic flow models are derived to facilitate simulating link traffic movement in a given lane i of the given incident-impacted link $\bar{l}$ with the relationships of lane-based speed–flow–density ($u-q-\rho$ for short) dynamics.

$$\rho_i^{\bar{l}}(x,t+\Delta t) = \rho_i^{\bar{l}}(x,t) + \frac{\Delta t}{\Delta x}\left[q_i^{\bar{l}}(x-\Delta x,t+\Delta t) - q_i^{\bar{l}}(x,t+\Delta t) + \Delta x\left(\sum_{\forall j} s_{j,i}^{\bar{l}}(x,t+\Delta t) - s_{i,j}^{\bar{l}}(x-\Delta x,t+\Delta t)\right)\right], \tag{10}$$

$$u_i^{\bar{l}}(x,t+\Delta t) = u_f\left[1 - \left(\frac{\rho_i^{\bar{l}}(x-\Delta x,t) + \rho_i^{\bar{l}}(x,t)}{2\rho_{jam}}\right)\right]^m, \tag{11}$$

$$q_i^{\bar{l}}(x,t+\Delta t) = \rho_i^{\bar{l}}(x,t+\Delta t) \times u_i^{\bar{l}}(x,t+\Delta t), \tag{12}$$

where Δx represents the length of a unit segment on the incident-impacted link $\bar{l}$; Δt is defined as the length of an unit time interval; u_f and ρ_{jam} correspond to the predetermined free-flow speed and the maximum-jam density, respectively; and m is a predetermined positive parameter.

2.3. Link cost calculation

In this mechanism, two types of link cost functions are involved, including incident-free and incident-impacted cost functions. Herein, the link travel time functions suggested in Ref. [41] are employed to calculate the incident-free link cost. By contrast, some modifications of the existing link cost functions are conducted for incident cases in consideration of the intra-lane and inter-lane traffic phenomena in the presence of incidents. The details of these models are described below.

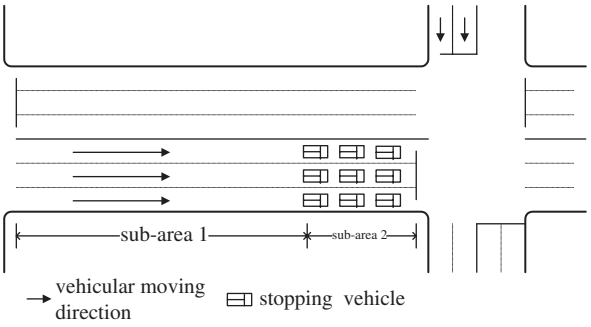

Fig. 4. Illustration of components of incident-free link travel time.

According to the models of Ran et al. [41], the incident-free link travel time contains two major parts: (1) cruising time in the main segment of a link, and (2) queuing delay at the approach of the given link, as illustrated in Fig. 4. Accordingly, the time-varying incident-free link travel time of a given incident-free link l ($\pi^l(t)$) in a given time interval t is given by

$$\pi^l(t) = \pi^l_{sub\text{-}1}(t) + \pi^l_{sub\text{-}2}(t), \tag{13}$$

where $\pi^l_{sub\text{-}1}(t)$ and $\pi^l_{sub\text{-}2}(t)$ represent the time-varying cruising time in the sub-area 1 (sub-1 for short) and (2) the average queuing delay in the sub-area 2 (sub-2 for short) of the given incident-free link l estimated in a given time interval t, respectively, and they are derived below.

Herein, $\pi^l_{sub\text{-}1}(t)$, which corresponds to the instantaneous average time spent by any given vehicle of sub-area 1 in running through the distance of sub-area 1 of the given incident-free link l, is estimated as follows. Given the number of vehicles queuing in sub-area 2 at the beginning of a given time interval t ($N^l_{sub\text{-}2}(t)$), the number of vehicles present in sub-area 2 at the end of the time interval t can be expressed as $N^l_{sub\text{-}2}(t) + [\alpha^l_{sub\text{-}2}(t) - \beta^l_{sub\text{-}2}(t)] \cdot \Delta t$, where $\alpha^l_{sub\text{-}2}(t)$ and $\beta^l_{sub\text{-}2}(t)$ represent the instantaneous arrival and departure rates of sub-area 2 of the given incident-free link l estimated in the given time interval t, respectively. By taking the average number of vehicles present in sub-area 2, divided by ρ_{jam} as the instantaneous length of sub-area 2 together with the aforementioned definition of $\pi^l_{sub\text{-}1}(t)$, we then have

$$\pi^l_{sub\text{-}1}(t) = 3600 \times \frac{L_l - \{N^l_{sub\text{-}2}(t) + \frac{1}{2}[\alpha^l_{sub\text{-}2}(t) - \beta^l_{sub\text{-}2}(t)] \times \Delta t\}/\rho_{jam}}{\bar{u}^l_{sub\text{-}1}(t)}, \tag{14}$$

where L_l represents the spatial length of the given incident-free link l; $\bar{u}^l_{sub\text{-}1}(t)$ is the instantaneous average speed observed in sub-area 1 of the given incident-free link l in the given time interval t.

Next, we take account of two types of delays in estimating $\pi^l_{sub\text{-}2}(t)$, including: (1) the stopping delay ($\delta^l_{stop}(t)$) and (2) the departure delay ($\delta^l_{dp}(t)$). The stopping delay ($\delta^l_{stop}(t)$) is primarily caused by the signal effect at the downstream intersection of the given incident-free link l in a given time interval t. Simply using Webster's delay equation, we estimate $\delta^l_{stop}(t)$ by

$$\delta^l_{stop}(t) = \frac{0.5 \times c^l_{dn}(t) \times [1 - g_{c^l_{dn}}(t)/c^l_{dn}(t)]^2}{1 - \theta_{c^l_{dn}}(t) \times g_{c^l_{dn}}(t)/c^l_{dn}(t)}, \tag{15}$$

where $c^l_{dn}(t)$ represents the cycle length of the intersection downstream (subscript dn for short) from the given incident-free link l observed in the given time interval t; $g_{c^l_{dn}}(t)$ represents the effective green time associated with $c^l_{dn}(t)$ observed in the given time interval t; $\theta_{c^l_{dn}}(t)$ represents the degree of saturation associated with $c^l_{dn}(t)$ in the incident-free link l observed in the given time interval t. The departure delay ($\delta^l_{dp}(t)$) is herein defined as the instantaneous average time spent in releasing the vehicles present in sub-area 2 of the given incident-free link l estimated in the given time interval t. Accordingly, $\delta^l_{dp}(t)$ is given by

$$\delta^l_{dp}(t) = 3600 \times \frac{[\alpha^l_{sub\text{-}2}(t) - \beta^l_{sub\text{-}2}(t)] \times \Delta t/2 + N^l_{sub\text{-}2}(t)}{\tilde{\mu}^l_{sub\text{-}2}(t)}, \tag{16}$$

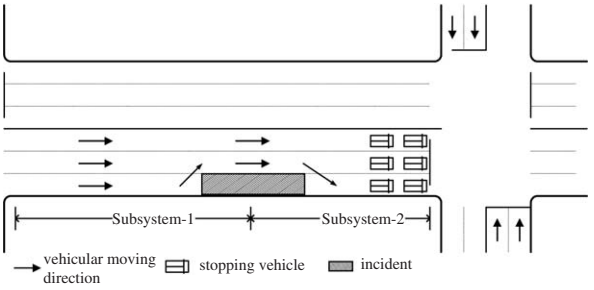

Fig. 5. Systems specification for incident-impacted link cost estimation.

where $\tilde{\mu}^{l}_{sub\text{-}2}(t)$ is the instantaneous saturation flow rate observed in sub-area 2 of the given incident-free link l in the given time interval t. Thus, utilizing Eqs. (15) and (16), $\pi^{l}_{sub\text{-}2}(t)$ is estimated by

$$\begin{aligned}\pi^{l}_{sub\text{-}2}(t) &= \delta^{l}_{stop}(t) + \delta^{l}_{dp}(t) \\ &= \frac{0.5 \times c^{l}_{dn}(t) \times [1 - g_{c^{l}_{dn}}(t)/c^{l}_{dn}(t)]^2}{1 - \theta_{c^{l}_{dn}}(t) \times g_{c^{l}_{dn}}(t)/c^{l}_{dn}(t)} + 3600 \times \frac{\{[\alpha^{l}_{sub\text{-}2}(t) - \beta^{l}_{sub\text{-}2}(t)] \times \Delta t/2 + N^{l}_{sub\text{-}2}(t)\}}{\tilde{\mu}^{l}_{sub\text{-}2}(t)}.\end{aligned} \tag{17}$$

In contrast with the aforementioned incident-free cases, the measure of dividing a link into two sub-areas remains in incident cases for link cost calculation, except for the boundaries of the two sub-areas. As we previously noted [3,4], two subsystems, namely subsystem 1 and subsystem 2, can be specified in a given incident-impacted link in consideration of the effects resulting from two different types of lane-changing maneuvers. As can be seen in Fig. 5, subsystem 1 geographically represents the area upstream from the incident site, aiming at the incident-induced mandatory lane changing from blocked lanes to adjacent lanes. In contrast, subsystem 2 situated downstream to the incident site is specified for the effect of discretionary lane changing from adjacent lanes to blocked lanes in that sub-area.

Based on the system specified above, the time-varying incident-impacted link cost function which is modified from the aforementioned incident-free link cost function is proposed as follows:

$$\pi^{\bar{l}}(t) = \pi^{\bar{l}}_{sub\text{-}1}(t) + \pi^{\bar{l}}_{sub\text{-}2}(t), \tag{18}$$

where $\pi^{\bar{l}}_{sub\text{-}1}(t)$ and $\pi^{\bar{l}}_{sub\text{-}2}(t)$ correspond to the average time spent, respectively, in subsystems 1 and 2 (sub-1 and sub-2 for short) of the incident-impacted link $\bar{l}$ estimated in a given time interval t.

Considering various types of delays caused by the intra-lane and inter-lane effects such as queuing and lane changing potentially present in subsystems 1 and 2, $\pi^{\bar{l}}_{sub\text{-}1}(t)$ and $\pi^{\bar{l}}_{sub\text{-}2}(t)$ are herein decomposed as

$$\pi^{\bar{l}}_{sub\text{-}1}(t) = \tau^{\bar{l}}_{sub\text{-}1}(t) + \delta^{\bar{l}}_{sub\text{-}1,que}(t) + \delta^{\bar{l}}_{sub\text{-}1,lane}(t), \tag{19}$$

$$\pi^{\bar{l}}_{sub\text{-}2}(t) = \tau^{\bar{l}}_{sub\text{-}2}(t) + \delta^{\bar{l}}_{sub\text{-}2,lane}(t) + \delta^{\bar{l}}_{sub\text{-}2,stop}(t) + \delta^{\bar{l}}_{sub\text{-}2,dp}(t). \tag{20}$$

As depicted in Eq. (19), the average time spent in subsystem 1 $\pi^{\bar{l}}_{sub\text{-}1}(t)$ includes three components: (1) the time-varying cruising time ($\tau^{\bar{l}}_{sub\text{-}1}(t)$), (2) the instantaneous average queuing delay ($\delta^{\bar{l}}_{sub\text{-}1,que}(t)$), and (3) the instantaneous average lane-changing time ($\delta^{\bar{l}}_{sub\text{-}1,lane}(t)$), where all the aforementioned items are estimated in subsystem 1 of the incident-impacted link $\bar{l}$ in the given time interval t. Similarly, in Eq. (2), the average time spent in subsystem 2 $\pi^{\bar{l}}_{sub\text{-}2}(t)$ is mainly composed of four items: (1) the time-varying cruising time ($\tau^{\bar{l}}_{sub\text{-}2}(t)$), (2) the instantaneous average discretionary lane-changing time ($\delta^{\bar{l}}_{sub\text{-}2,lane}(t)$), (3) the instantaneous average stopping delay caused by the signal control effect ($\delta^{\bar{l}}_{sub\text{-}2,stop}(t)$), and (4) the instantaneous average departure delay ($\delta^{\bar{l}}_{sub\text{-}2,dp}(t)$) referring to the instantaneous average time spent in releasing the vehicles stopped at the downstream intersection of the incident-impacted link $\bar{l}$, where all the aforementioned items are estimated in subsystem 2 of the incident-impacted link $\bar{l}$ in the given time interval t. Herein, the aforementioned items of

$\pi^{\bar{l}}_{sub\text{-}1}(t)$ and $\pi^{\bar{l}}_{sub\text{-}2}(t)$ are given by

$$\pi^{\bar{l}}_{sub\text{-}1}(t) = 3600 \times \frac{L^{\bar{l}}_{sub\text{-}1} - \{N^{\bar{l}}_{sub\text{-}1}(t) + \frac{1}{2}[\alpha^{\bar{l}}_{sub\text{-}1}(t) - \beta^{\bar{l}}_{sub\text{-}1}(t)]\Delta t\}/\rho_{jam}}{\bar{u}^{\bar{l}}_{sub\text{-}1}(t)}, \tag{21}$$

$$\delta^{\bar{l}}_{sub\text{-}1,que}(t) = 3600 \times \frac{N^{\bar{l}}_{sub\text{-}1}(t) + \frac{1}{2}[\alpha^{\bar{l}}_{sub\text{-}1}(t) - \beta^{\bar{l}}_{sub\text{-}1}(t)] \times \Delta t}{\tilde{\mu}^{\bar{l}}_{sub\text{-}1}(t)}, \tag{22}$$

$$\begin{aligned}\delta^{\bar{l}}_{sub\text{-}1,lane}(t) &= \frac{\{N^{\bar{l}}_{sub\text{-}1}(t) \times ave[p^{\bar{l}_{mc}}_{i,j}(x,t)] \times \bar{t}_{mc}\} + \{N^{\bar{l}}_{sub\text{-}1}(t) \times ave[p^{\bar{l}_{dc}}_{i,j}(x,t)] \times \bar{t}_{dc}\}}{N^{\bar{l}}_{sub\text{-}1}(t)} \\ &= ave[p^{\bar{l}_{mc}}_{i,j}(x,t)] \times \bar{t}_{mc} + ave[p^{\bar{l}_{dc}}_{i,j}(x,t)] \times \bar{t}_{dc},\end{aligned} \tag{23}$$

$$\pi^{\bar{l}}_{sub\text{-}2}(t) = 3600 \times \frac{L^{\bar{l}}_{sub\text{-}2} - \{N^{\bar{l}}_{sub\text{-}2}(t) + \frac{1}{2}[\alpha^{\bar{l}}_{sub\text{-}2}(t) - \beta^{\bar{l}}_{sub\text{-}2}(t)] \times \Delta t\}/\rho_{jam}}{\bar{u}^{\bar{l}}_{sub\text{-}2}(t)}, \tag{24}$$

$$\delta^{\bar{l}}_{sub\text{-}2,lane}(t) = \frac{N^{\bar{l}}_{sub\text{-}2}(t) \times ave[p^{\bar{l}_{dc}}_{i,j}(x,t)] \times \bar{t}_{dc}}{N^{\bar{l}}_{sub\text{-}2}(t)} = ave[p^{\bar{l}_{dc}}_{i,j}(x,t)] \times \bar{t}_{dc}, \tag{25}$$

$$\delta^{\bar{l}}_{sub\text{-}2,stop}(t) = \frac{0.5 \times c^{\bar{l}}_{dn}(t) \times [1 - g_{c^{\bar{l}}_{dn}}(t)/c^{\bar{l}}_{dn}(t)]^2}{1 - \theta_{c^{\bar{l}}_{dn}}(t) \times g_{c^{\bar{l}}_{dn}}(t)/c^{\bar{l}}_{dn}(t)}, \tag{26}$$

$$\delta^{\bar{l}}_{sub\text{-}2,dp}(t) = 3600 \times \frac{[\alpha^{\bar{l}}_{sub\text{-}2}(t) - \beta^{\bar{l}}_{sub\text{-}2}(t)] \times \Delta t/2 + N^{\bar{l}}_{sub\text{-}2}(t)}{\tilde{\mu}^{\bar{l}}_{sub\text{-}2}(t)}, \tag{27}$$

where $L^{\bar{l}}_{sub\text{-}1}$ and $L^{\bar{l}}_{sub\text{-}2}$ denote the spatial lengths of subsystems 1 and 2 of the given incident-impacted link $\bar{l}$, respectively; $N^{\bar{l}}_{sub\text{-}1}(t)$ and $N^{\bar{l}}_{sub\text{-}2}(t)$ represent the numbers of vehicles present in subsystems 1 and 2 in a given time interval t, respectively; $ave[p^{\bar{l}_{dc}}_{i,j}(x,t)]$ and $ave[p^{\bar{l}_{mc}}_{i,j}(x,t)]$ represent the instantaneous averaged values of the corresponding discretionary and mandatory lane-changing probabilities (i.e., $p^{\bar{l}_{dc}}_{i,j}(x,t)$ and $p^{\bar{l}_{mc}}_{i,j}(x,t)$) in a given time interval t; $\alpha^{\bar{l}}_{sub\text{-}1}(t)$ and $\beta^{\bar{l}}_{sub\text{-}1}(t)$ are the arrival and departure rates of subsystem 1 measured in a given time interval t; similarly, $\alpha^{\bar{l}}_{sub\text{-}2}(t)$ and $\beta^{\bar{l}}_{sub\text{-}2}(t)$ are the measured arrival and departure rates of subsystem 2 in a given time interval t; $\bar{u}^{\bar{l}}_{sub\text{-}1}(t)$ and $\bar{u}^{\bar{l}}_{sub\text{-}2}(t)$ represent the instantaneous average speeds observed in subsystems 1 and 2 of the given incident-impacted link $\bar{l}$ in the given time interval t; $\tilde{\mu}^{\bar{l}}_{sub\text{-}1}(t)$ and $\tilde{\mu}^{\bar{l}}_{sub\text{-}2}(t)$ represent the instantaneous saturation flow rates observed in subsystems 1 and 2 of the given incident-impacted link $\bar{l}$ in the given time interval t, respectively; $\bar{t}_{mc}$ and $\bar{t}_{dc}$ represent the average time needed, respectively, for conducting the mandatory and discretionary lane-changing maneuvers, both of which are assumed to be time-invariant for model simplification. In addition, the definitions of the signal control parameters including $c^{\bar{l}}_{dn}(t)$, $g_{c^{\bar{l}}_{dn}}(t)$ and $\theta_{c^{\bar{l}}_{dn}}(t)$ remain the same as those defined for incident-free cases, given that they are associated with the downstream intersection of the given incident-impacted link $\bar{l}$.

2.4. Searching the shortest path

This mechanism aims to find the instantaneous shortest paths for reloading vehicles approaching from each given node to the following links of the simulation-assignment network in the next time interval $k+1$. Herein, the well-known label-correcting algorithm, together with the time-varying link costs estimated in the previous

mechanism, is employed to determine the instantaneous shortest-path trees from each given origin to all the destinations in the specified simulation-assignment network. Correspondingly, the primary procedures executed in the conventional label-correcting approach almost remains in this mechanism except the determination of the link-cost component of a label associated with each node. Utilizing classical label-correcting approaches, the link-cost component of a label is set to be constant, and predetermined according to the static node-to-node distance. By contrast, the proposed algorithm updates the link-cost components of labels in each time interval using the time-varying link costs estimated in the previous mechanism in response to the dynamics of link traffic flows as well as the incident-induced traffic congestion in the process of DTA. The major computational steps performed in this mechanism are summarized as follows.

Step 1: Update the link travel time associated with each link of the simulation-assignment network using the time-varying link costs estimated in the given time interval k in the previous mechanism.

Step 2: Given one origin $\tilde{O}$ labeled with $(0, \tilde{O})$, specify a temporary label $(\pi_{\tilde{O},m}(k), \tilde{O})$ associated with each downstream node m that is directly connected to $\tilde{O}$, where the first component of the label $\pi_{\tilde{O},m}(k)$ denotes the time-varying path travel time from the given origin $\tilde{O}$ to the given downstream node m in a given time interval k.

Step 3: Of all nodes with temporary labels, choose one whose time-varying path travel time exhibited in the associated label is minimal, and declare that node to be permanently labeled. Note that at any point in this step any ties may be arbitrarily broken. As soon as all nodes are coded with permanent labels, go to Step 5. Otherwise, go to the next step (i.e., Step 4).

Step 4: Let m^* denote the last node whose label has been declared permanent, and consider all the downstream nodes that are directly connected to m^*. For each such node n, compute the sum of its time-varying link travel time to m^* plus the first component exhibited in the label of m^*. If the given downstream node n is unlabeled, assign a temporary label consisting of the summed path travel time as the first component, and m^* as the second component of the temporary label associated with the given downstream node n. If the given downstream node n already has a temporary label, and the newly calculated path travel time is less than the first component of the temporary label, update the first component of the temporary label with the newly calculated path travel time. Then go back to Step 3.

Step 5. If all origins of the network have been considered, terminate the shortest-path searching procedure in the given time interval k. Otherwise, go back to Step 2 to continue the searching procedure.

Note that the permanent labels indicate the shortest path from one given origin to each node in the simulation-assignment network, and also indicate the preceding node on the shortest path to each node. Using this mechanism, an instantaneous turning-moving decision can be made for each vehicle approaching a given node in the given time interval k for the routine of link flow loading executed in the next time interval $k+1$.

3. Numerical examples

This numerical study investigates the potential advantages of the proposed simulation-based DTA method with respect to responding in real time to diverse blocking cases on surface streets, compared with previous simulation-based DTA algorithms. The proposed algorithm was coded in Turbo C. Employing specific criteria, the proposed method was compared with the Paramics microscopic traffic simulator, which embeds several elaborate traffic assignment models including stochastic assignment and dynamic feedback assignment as well as combining assignment techniques, to evaluate the DTA performance under various lane-blocking incident conditions. Both the proposed algorithm and Paramics were run on a personal computer at 233 MHz. Descriptions of calibrating and testing the Paramics simulator can also be found elsewhere [48]. The details in relation to the traffic assignment functions built in Paramics can also be found elsewhere [49], and thus are omitted in this section.

A simple grid-shaped traffic network comprising nine intersections was simulated. Fig. 6 illustrates the scheme of the study network, where each node represents an intersection coded with a specific integer value for its identification, and controlled with predetermined two-phase fixed timing schemes. The primary parameters set for simulation are summarized in Table 1.

Given the aforementioned simulation parameters, a total of nine lane-blocking incident scenarios associated with diverse incident-related attributes, including traffic flow conditions, incident duration and location were

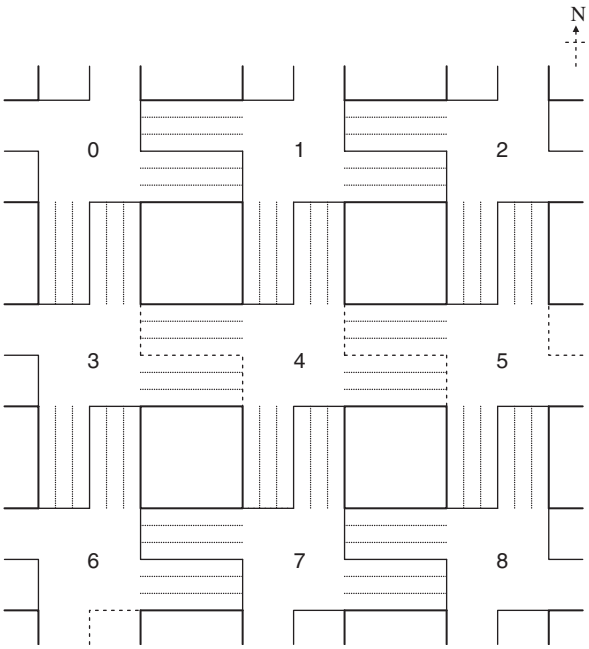

Fig. 6. The simulated network.

Table 1
The primary parameters preset for simulation

1. *Geometric characteristics*	
(1) Link attributes	
(a) Number of links	24
(b) Length of link (m)	300
(c) Number of lanes on each link	3
(d) Lane width (m)	4
(2) Node attributes	
Number of nodes	9
2. *Signal control characteristics*	
(1) Cycle length for each intersection (s)	150
(2) Number of phases	2
(3) Green/red interval for phase 1 (s)	80/70
(4) Green/red interval for phase 2 (s)	70/80
3. *Operational characteristics of simulation*	
(1) Simulation duration (s)	3600
(2) Update frequency (time/s)	1

simulated in the network. Table 2 presents the specific simulation characteristics of the nine test scenarios, classified briefly into the aforementioned three types of incident characteristics. Here, the traffic arrivals entering the network are assumed to follow Poisson processes, and generated using different mean values in different test scenarios. The total hourly O–D flow shown in Table 2 refers to the network-wide traffic flow generated for testing in a given 1-h simulation case.

To demonstrate the relative advantages of the proposed method with respect to the improvements in network-wide traffic assignment performance under diverse incident conditions in comparison with Paramics, three evaluation measures are utilized: (1) network-wide average path travel time ($\overline{AI}$), (2) average density-based incident-impact index ($\overline{DI}$), and (3) average volume-based incident-impact index ($\overline{VI}$). Herein, $\overline{DI}$ and

Table 2
Simulation characteristics of test scenarios

Characteristics	Test scenario (coded with S-"i" for short)								
	Traffic flow condition			Incident duration			Incident location (relative to the network)		
	S-1 (high)	S-2 (medium)	S-3 (low)	S-4 (long)	S-5 (medium)	S-6 (short)	S-7 (start)	S-8 (central)	S-9 (end)
Total hourly O–D flow (veh/h)	7500	5000	2500	5000	5000	5000	5000	5000	5000
Incident-located link (node–node)	3–4	3–4	3–4	3–4	3–4	3–4	0–3	3–4	7–8
Incident duration (min)	10	10	10	30	10	3	10	10	10

$\overline{VI}$ are two measures proposed particularly for assessing the improvements in terms of incident impact, and they are denoted as

$$\overline{DI} = \frac{\sum_{t=1}^{T_{\bar{l}}} DI(t)}{T_{\bar{l}}}, \tag{28}$$

$$\overline{VI} = \frac{\sum_{t=1}^{T_{\bar{l}}} VI(t)}{T_{\bar{l}}}, \tag{29}$$

where $DI(t)$ and $VI(t)$ represent the time-varying density-based and volume-based incident-impacts which were proposed in our previous research [46] for assessing the severity of incident impact in the spatial domain, and are herein given by

$$DI(t) = \frac{N^{\bar{l}}_{sub\text{-}1}(t)}{L^{\bar{l}}_{sub\text{-}1}}, \tag{30}$$

$$VI(t) = \frac{N^{\bar{l}}_{sub\text{-}1}(t)}{N^{\bar{l}}_{sub\text{-}1}(t) + N^{\bar{l}}_{sub\text{-}2}(t)}. \tag{31}$$

The numerical results of comparisons are summarized in Tables 3–5, classified by the attributes of traffic flow conditions, incident location, and incident duration, respectively. Several findings observed in the numerical study are provided as follows for further discussion.

From Table 3, it can be seen that the in-vehicle RG proposed method appears to perform relatively better under low-volume traffic conditions than under high-volume conditions, for minimizing either the network-wide path travel time or the incident impact on link traffic flows. This implies that the problem of incident-induced traffic congestion under high-volume traffic conditions remains to be solved in both the fields of DTA and incident management. Accordingly, integration with other related traffic control strategies, e.g., advanced incident-responsive signal control technologies, may warrant further investigation to address this issue.

With regard to the effect of incident duration on system performance, it can be induced from the results of Table 4 that the proposed method does not seem to be affected by this effect. Such a generalization is consistent with our prior speculation that an appropriate incident-responsive route choice algorithm must perform stably regardless of incident duration. As can be seen in Table 4, the proposed method appears to have the quick response capability for short-term incident events, e.g. 3 min lane-blocking incidents in the test scenario under which the incident impact seems to be reduced to a greater extent in comparison with the other incident-duration cases, regardless of the corresponding higher average path travel time ($\overline{AI}$).

In contrast with the effect of incident duration, the numerical results presented in Table 4 explore the effect of incident location on DTA performance. Here, it is observed that the incident-location effect is not significant for the proposed DTA method. However, by comparison, the performance of Paramics appears to

Table 3
Comparison results (by traffic flow conditions)

Evaluation measure	Test scenario		
	S-1 (High-volume)	S-2 (Medium-volume)	S-3 (Low-volume)
$\overline{AI}$			
Paramics (s)	187.99	184.82	180.79
IR-RG (s)	180.01	162.44	153.24
Relative improvement (%)	4.24	12.11	15.24
$\overline{DI}$			
Paramics	0.075	0.042	0.025
IR-RG	0.018	0.009	0.004
Relative improvement (%)	76.00	78.57	84.00
$\overline{VI}$			
Paramics	0.614	0.666	0.775
IR-RG	0.444	0.349	0.198
Relative improvement (%)	27.69	47.60	74.45

Table 4
Comparison results (by incident duration)

Evaluation measure	Test scenario (incident-duration)		
	S-4 (long)	S-5 (medium)	S-6 (short)
$\overline{AI}$			
Paramics (s)	187.32	184.82	184.29
IR-RG (s)	163.34	162.44	164.35
Relative improvement (%)	12.80	12.11	10.82
$\overline{DI}$			
Paramics	0.043	0.042	0.036
IR-RG	0.009	0.009	0.006
Relative improvement (%)	79.07	78.57	83.33
$\overline{VI}$			
Paramics	0.639	0.666	0.615
IR-RG	0.328	0.349	0.222
Relative improvement (%)	48.67	47.60	63.90

be affected by this effect, particularly under the condition of incidents located near the destinations of the network, as can be observed in the scenario of S-9 in Table 5.

Overall, the comparison results summarized above indicate the relative advantages of the proposed method with respect to improvement in the DTA performance under various lane-blocking incident conditions in comparison with the Paramics simulator, e.g., the reductions in network-wide path travel time by 11.4%, and by 66.7% with respect to incident impact alleviation. Such a generalization is not surprising because the proposed method dynamically accommodates the time-varying estimates of incident-induced link costs in the DTA procedure in response to the incident impact either spatially or temporally on network-wide traffic movements. In contrast, most existing algorithms, including these advanced traffic assignment models embedded in Paramics, may not involve such specific traffic assignment logic and link cost functions for incident cases, and thus may lead to inferior solutions, as displayed in the numerical results.

Table 5
Comparison results (by incident location)

Evaluation measure	Test scenario (incident-location relative to the network)		
	S-7 (start)	S-8 (central)	S-9 (end)
$\overline{AI}$			
Paramics (s)	183.97	184.82	187.17
IR-RG (s)	164.17	162.44	163.88
Relative improvement (%)	10.76	12.11	12.44
$\overline{DI}$			
Paramics	0.043	0.042	0.064
IR-RG	0.006	0.009	0.014
Relative improvement (%)	86.05	78.57	78.13
$\overline{VI}$			
Paramics	0.639	0.666	0.900
IR-RG	0.261	0.349	0.342
Relative improvement (%)	59.15	47.60	62.00

Table 6
Comparison results for illustration of incident-induced lane-changing effects on traffic assignment

Evaluation measure	Link traffic flow condition		
	High-volume	Medium-volume	Low-volume
$\overline{AI}$ (s)			
The proposed model	93.2	75.6	53.7
Basic LWR model	96.7	82.4	69.2
Relative improvement (%)	3.76	8.99	28.9

In addition, to further illustrate the importance of involving incident-induced lane-changing models in decision-making of traffic assignment, we have added a simplified numerical example with testing our proposed method embedding two different link flow models, referring, respectively, to the proposed modified LWR model with the consideration of lane-changing formulas, and the basic LWR model. In this test scenario, a simple network consisting of two nodes connecting with two identical 3-lane links was built. Then a total of 30 10 min lane-blocking incidents were simulated on one of the given two links with three preset traffic flow conditions, e.g., low-volume, medium-volume, and high-volume cases. Here, the average path travel time ($\overline{AI}$) remains used as the assessment measure. The numerical results are summarized in Table 6.

According to the corresponding test results shown in Table 6, the improvement of the proposed hybrid link flow model in terms of average path travel time seems to be relatively significant in both low-volume and medium incident cases, compared to the high-volume case. In reality, such numerical results are consistent with the generalizations obtained from Table 3, which have implied the relatively high performance of the proposed method under low-volume incident conditions. However, compared to the LWR model, which does not consider incident-induced lane-changing maneuvers on the incident link, the proposed incident-induced link flow model may still exhibit its relatively high feasibility for responding to incident impacts on link traffic flows in the DTA decision-making process. According to our observations from the tests, the corresponding relative advantage of the proposed model results from its capability of approximating time-varying incident-impacted link travel time, and dynamically responding to the corresponding incident impact on link traffic flows. For instance, under the low-volume incident condition, the proposed link flow model tends to divert less vehicles to the incident-free lane than the basic LWR model did because the corresponding incident impact in the low-volume incident case is less than that of the high-volume incident case. In contrast, under high-volume

incident condition, the corresponding performance of the proposed model turns out to be relatively limited because both the incident-free and incident-impacted links have almost reached to their link capacities in the traffic assignment process.

4. Concluding remarks

This paper has presented a simulation-based approach to address the issue of DTA in the presence of lane-blocking incidents on surface streets. The proposed in-vehicle RG method primarily involves four mechanisms that are sequentially executed to deal with network-wide link traffic flows moving in both incident-free and incident-impacted links, ensuring that each vehicle keeps moving on the associated time-varying instantaneous shortest path before arriving at its destination. To account for the incident effect on link travel time in the traffic assignment procedure, specific incident-impacted link cost functions that characterize incident-induced inter-lane and intra-lane traffic phenomena are formulated.

The proposed algorithm is tested with nine different simulated lane-blocking incident scenarios, and the performance is compared with the Paramics microscopic traffic simulator. Overall, the numerical results indicate the superiority of the proposed method, which reduces both the network-wide path travel time by 11.4% and the incident impact on link traffic flows by 66.7% in the process of DTA under various lane-blocking incident conditions, as compared with Paramics.

Despite these potential advantages mentioned above, further tests and modifications may be needed to verify the robustness of the proposed incident-responsive in-vehicle RG method, and its applicability to diverse incident cases on surface streets, such as queue overflows and gridlocks. Modeling testing with large-scale traffic assignment networks is particularly needed to investigate the computational performance of the proposed method for real-time applications. Coordination with advanced signal control technologies responding in real time to diverse incident impacts on network-wide traffic congestion also warrants further research.

In addition, such relative competitiveness of the proposed method mentioned above may suggest the potential of applying the proposed model in guiding vehicles moving smoothly from certain origins to destinations in a given network in real time for the case of surface street incidents. Thus, the incident effects on road traffic congestion could be alleviated to a great extent using advanced ITS technologies such as RG systems, coupled with appropriate incident-responsive traffic control and management strategies. More importantly, it is expected that this study provides a linkage between the areas of DTA and incident management, and also may stimulate more research in related fields.

Acknowledgements

This research was supported by the grant NSC 94-2416-H-009-009 from the National Science Council of Taiwan. The author would also like to thank the referees for their constructive comments. Any errors or omissions remain the sole responsibility of the authors.

References

[1] J.M. Morales, Analytical procedures for estimating freeway traffic congestion, Public Road 50 (2) (1986) 55–61.
[2] H. Al-Deek, A. Garib, A.E. Radwan, Methods for estimating freeway incident congestion, Presented at Transportation Research Board, 74th Annual Meeting, Washington, DC, 1995.
[3] J.-B. Sheu, Y.-H. Chou, L.-J. Shen, A stochastic estimation approach to real-time prediction of incident effects on freeway traffic congestion, Transp. Res. B 35B (6) (2001) 575–592.
[4] J.-B. Sheu, S.G. Ritchie, Stochastic modeling and real-time prediction of vehicular lane-changing behavior, Transp. Res. B 35B (7) (2001) 695–716.
[5] C.F. Daganzo, Queue spillovers in transportation networks with a route choice, Transp. Sci. 32 (1998) 3–11.
[6] D.K. Merchant, G.L. Nemhauser, A model and an algorithm for the dynamic traffic assignment problems, Transp. Sci. 12 (1978) 183–199.
[7] D.K. Merchant, G.L. Nemhauser, Optimality conditions for a dynamic traffic assignment model, Transp. Sci. 12 (1978) 200–207.
[8] M. Carey, Optimal time-varying flows on congested network, Oper. Res. 35 (1987) 58–69.

[9] B.N. Janson, J. Robles, Dynamic traffic assignment with arrival time costs, in: C.F. Daganzo (Ed.), Proceedings of the 12th International Symposium on Transportation and Traffic Theory, Berkeley, Elsevier, New York, 1993, pp. 127–146.
[10] G. Ziyou, S. Yifan, A reserve capacity model of optimal signal control with user-equilibrium route choice, Transp. Res. B 36B (4) (2002) 313–323.
[11] F.J. Luque, T.L. Friesz, Dynamic traffic assignment considered as a continuous time optimal control problem, Paper presented at the TIMS/ORSA Joint National Meeting, Washington, DC, May 5–7, 1980.
[12] T.L. Feiesz, F.J. Luque, R.L. Tobin, B.W. Wei, Dynamic network traffic assignment considered as a continuous time optimal control problem, Oper. Res. 37 (1989) 893–901.
[13] N.H. Gartner, G. Improta, Editorial for special issue on urban traffic networks: dynamic control and flow equilibrium, Transp. Res. B 24B (1990) 407–408.
[14] M. Papageorgiou, Dynamic modeling, assignment, and route guidance in traffic network, Transp. Res. B 24B (1990) 471–495.
[15] B. Ran, T. Shimazaki, Dynamic user equilibrium traffic assignment for congested transportation networks, Paper presented at the Fifth World Conference on Transport Research, Yokohama, Japan, 1989
[16] B.W. Wei, An application of optimal control theory to dynamic user equilibrium traffic assignment, Transp. Res. Rec. 1251 (1989) 66–73.
[17] B.W. Wei, T.L. Friesz, R.L. Tobin, Dynamic user optimal traffic assignment on congested multidestination networks, Transp. Res. B 24B (1990) 431–442.
[18] D.E. Boyce, B. Ran, L.J. LeBlanc, Solving an instantaneous dynamic user-optimal route choice model, Transp. Sci. 29 (1993) 128–142.
[19] B. Ran, D.E. Boyce, L.J. LeBlanc, A new class of instantaneous dynamic user-optimal assignment models, Oper. Res. 41 (1993) 192–202.
[20] T.L. Friesz, D. Bernstein, T.E. Smith, R.L. Tobin, B.W. Wei, A variational inequality formulation of the dynamic network user equilibrium problem, Oper. Res. 41 (1993) 179–191.
[21] M.J. Smith, A new dynamic traffic model and the existence and calculation of dynamic user equilibrium on congested capacity-constrained road networks, Transp. Res. B 27B (1993) 49–63.
[22] B.W. Wie, R.L. Tobin, D. Bernstein, T.R. Freisz, A comparison of system equilibrium dynamic traffic assignments with schedule delays, Transp. Res. C 3 (6) (1995) 381–411.
[23] B. Ran, D.E. Boyce (Eds.), Modeling dynamic transportation networks: an intelligent transportation system oriented approach, Springer, New York, 1996.
[24] H.-K. Chen, C.-F. Hsueh, A model and an algorithm for the dynamic user-optimal route choice problem, Transp. Res. B 32B (3) (1998) 219–234.
[25] H.-J. Cho, T.E. Smith, T.L. Friesz, A reduction method for local sensitivity analysis of network equilibrium arc flows, Transp. Res. B 34B (1) (2000) 31–51.
[26] H.-J. Huang, W.H.K. Lam, Modeling and solving the dynamic user equilibrium route and departure time choice problem in network with queues, Transp. Res. B 36B (3) (2002) 253–273.
[27] D.R. Leonard, P. Gower, N.B. Tayler, CONTRAM: structure of the model, Transport and Road Research Laboratory Report RR178, Crowthorne, UK, 1989.
[28] N.B. Tayler, CONTRAM 5: an enhanced traffic assignment model, Transport and Research Laboratory Report RR249, Crowthorne, UK, 1990.
[29] M. Van Aerde, S. Yagar, Dynamic integrated freeway/traffic signal networks: a routing-based modeling approach, Transp. Res. A 22A (1988) 445–453.
[30] H.S. Mahmassani, T.Y. Hu, R. Jayakrishnan, Dynamic traffic assignment and simulation for advanced network informatics (DYNASMART), Proceedings of the Second International Capri Seminar on Urban Traffic Networks, Capri, Italy, 1992.
[31] R. Jayakrishnan, H.S. Mahmassani, T.Y. Hu, An evaluation tool for advanced traffic information and management systems in urban networks, Transp. Res. C 2C (1994) 129–147.
[32] R. Jayakrishnan, W.K. Tsai, J.N. Prashker, S. Rajadhyaksha, Faster path-based algorithm for traffic assignment, Transp. Res. Rec. 1443 (1994) 75–83.
[33] T.-Y. Hu, H.S. Mahmassani, Day-to-day evolution of network flows under real-time information and reactive signal control, Transp. Res. C 5C (1) (1997) 51–69.
[34] M.O. Ghali, M.J. Smith, Traffic assignment, traffic control and road pricing, Proceedings of the 12th International Symposium on Transportation and Traffic Theory, Elsevier Science Publishers B.V., Amsterdam, 1993, pp. 147–169.
[35] M.O. Ghali, M.J. Smith, Comparisons of the performances of three responsive traffic control policies, taking drivers' day-to-day route-choices into account, Traffic Eng. Control 35 (10) (1994) 555–560.
[36] M.O. Ghali, M.J. Smith, Designing time-of-day signal plans which reduce urban traffic congestion, Traffic Eng. Control 35 (12) (1994) 672–676.
[37] M. Ben-Akiva, A. Palma, P. Kanaroglou, Dynamic model of peak period traffic congestion with elastic arrival rates, Transp. Sci. 20 (1986) 164–181.
[38] N.B. Hounsell, M. McDonald, L. Breheret, Models and strategies for dynamic route guidance, in: Commission of the European Communities, Directorate-General, Telecommunications, Information Industries, and Innovation (Eds.), Advanced Telematics in Road Transport: Proceedings of the DRIVE Conference, Elsevier, Brussels, February 4–6, 1991, pp. 89–98.
[39] C.O. Tong, S.C. Wong, A predictive dynamic traffic assignment model in congested capacity-constrained road networks, Transp. Res. B 34B (2000) 625–644.

[40] M. Rickert, K. Nagel, Traffic simulation: dynamic traffic assignment on parallel computers in TRANSIMS, Future Generation Comput. Syst. 17 (2001) 637–648.
[41] B. Ran, N.M. Rouphail, A. Tapko, D.E. Boyce, Toward a class of link travel time functions for dynamic assignment models on signalized networks, Transp. Res. B 31B (1997) 277–290.
[42] M.G.M. Bell, W.H.K. Lam, Y. Iida, A time-dependent multi-class path flow estimator, in: J.-B. Lesort (Ed.), Proceedings of the 13th International Symposium on Transportation and Traffic Theory, Elsevier, Amsterdam, 1996, pp. 173–194.
[43] W.H.K. Lam, Y.P. Zhang, Y.F. Yin, Time-dependent model for departure time and route choices in networks with queues, Transp. Res. Rec. 1667 (1999) 33–41.
[44] A. Chen, D.H. Lee, Path-based algorithms for large scale traffic equilibrium problem: a comparison between DSD and GP, Presented at Transportation Research Board, 78th Annual Meeting, Washington, DC, 1998.
[45] M.J. Lighthill, G.B. Whitham, On kinematics waves II: a theory of traffic flow on long crowded road, Proceedings of the Royal Society, A229, London, UK, 1955, pp. 317–345.
[46] J.-B. Sheu, Y.-H. Chou, A. Chen, Stochastic modeling and real-time estimation of incident effects on surface street traffic congestion, Appl. Math. Modelling 28 (5) (2004) 445–468.
[47] M. Ben-Akiva, S.R. Lerman, Discrete Choice Analysis: Theory and Application to Travel Demand, The MIT Press, Massachusetts, 1985.
[48] B. Abdulhai, J.-B. Sheu, W.W. Recker, Simulation of ITS on the Irvine FOT area using the 'Paramics 1.5' scalable microscopic traffic simulator: phase I: model calibration and validation, California PATH Research Report UCB-ITS-PRR-99-12 1055-1425, 1999.
[49] Quadstone Ltd., Paramics Traffic Simulation, Modeller V3.0, User Guide, 2000.